Within hierarchical cosmological scenario, clusters
Are though to form through the merger of smaller systems, likely at the intersection of the large scale structure (LSS).

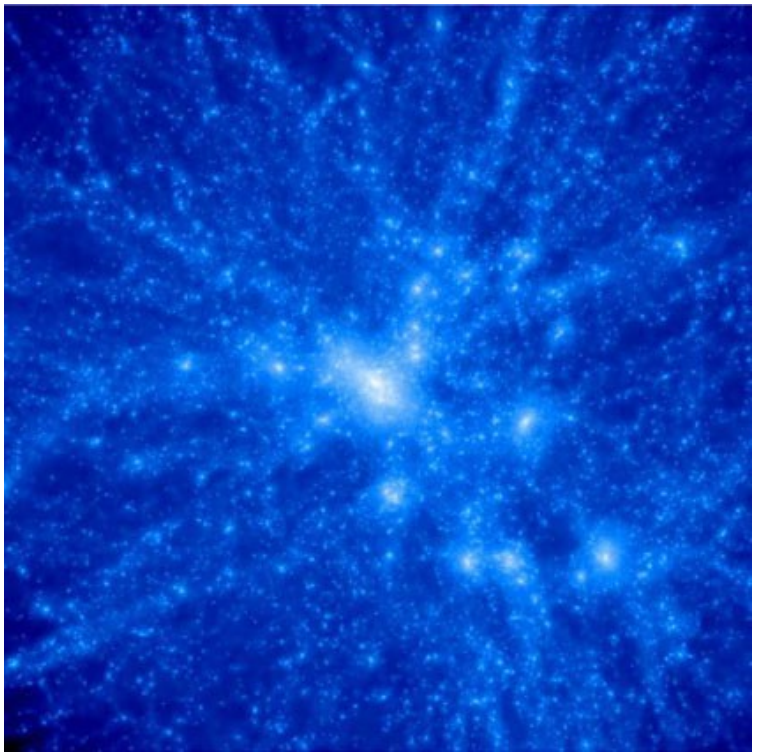

Kravtov & Borgani 2012
A&A Annual Review 12

Cluster merger is an ongoing process, with a lot of
observational evidence in both local and distant Universe.
A connected feature is the presence of SUBSTRUCTURE.

OPTICAL STUDIES FROM GALAXIES >50%
of clusters show substructure
(small substructure ~10% of the total mass)
Major substructure (=major merger) only in 10% of clusters.

Methods of detection:
1D in the velocity space
2D gals density onto the sky
3D correlation between position and velocity

SUBSTRUCTURE MAY BE:
*cluster mergers,
*subsystems with system already relaxed (remnant),
*bound group that will merge,
*unbound group, projected onto the cluster.

2D analysis.
Galaxy density isocontours.

Geller 1982.
For a local cluster.

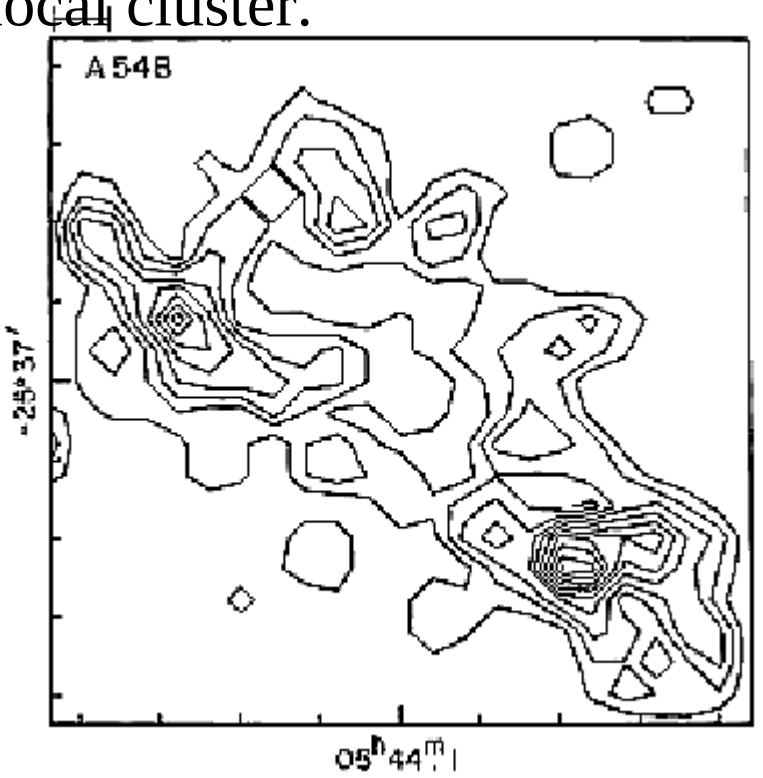

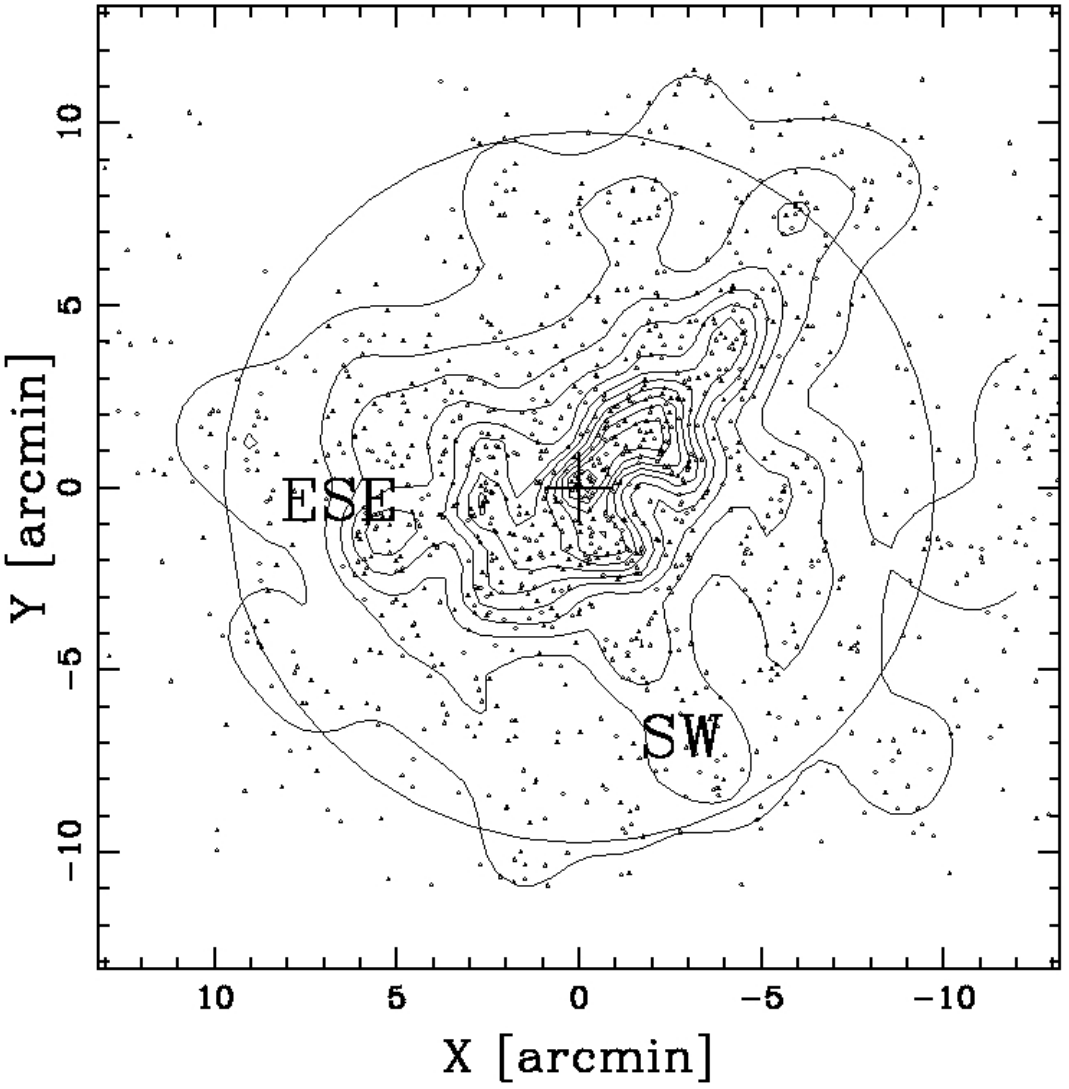

Ongoing work on Abell 209
CLASH-VLT data for >1000 gals
At z=0.2. 1116 cluster gals.
PI Piero Rosati.
In TS, MG,A.Biviano,M.Nonino,
+others and postdocs

Since the violent relaxation theory → Gaussian 1D velocity distribution

1D – tests often based on Gaussian.

This is instead the result for a non-parametric adaptive method of galaxy density.

A 10% OF CLUSTERS ARE FAR FROM DYNAMICAL EQUILIBRIUM → MASS ESTIMATE VARIES BY A FACTOR 2

σv estimate increases during the merger!

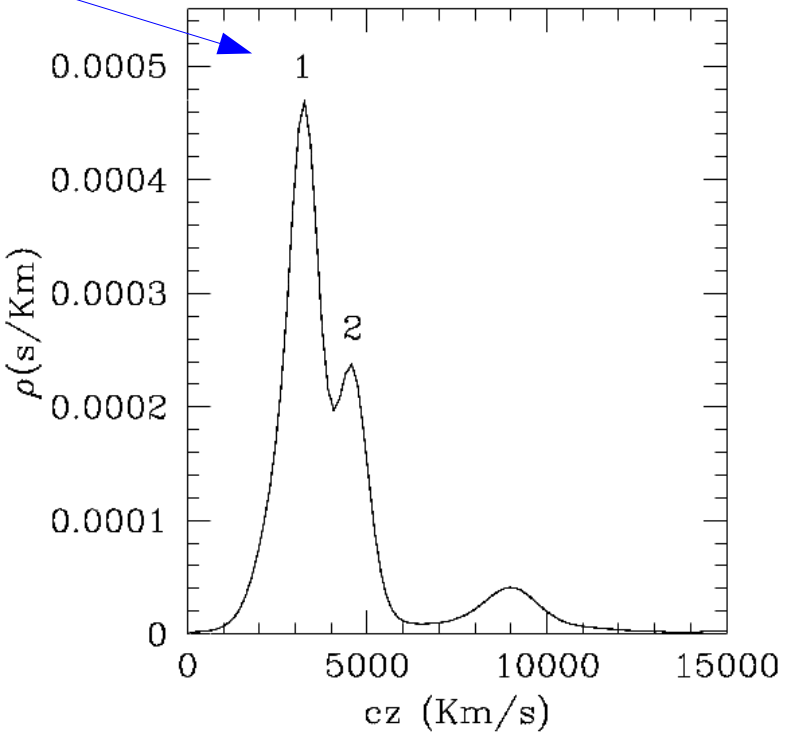

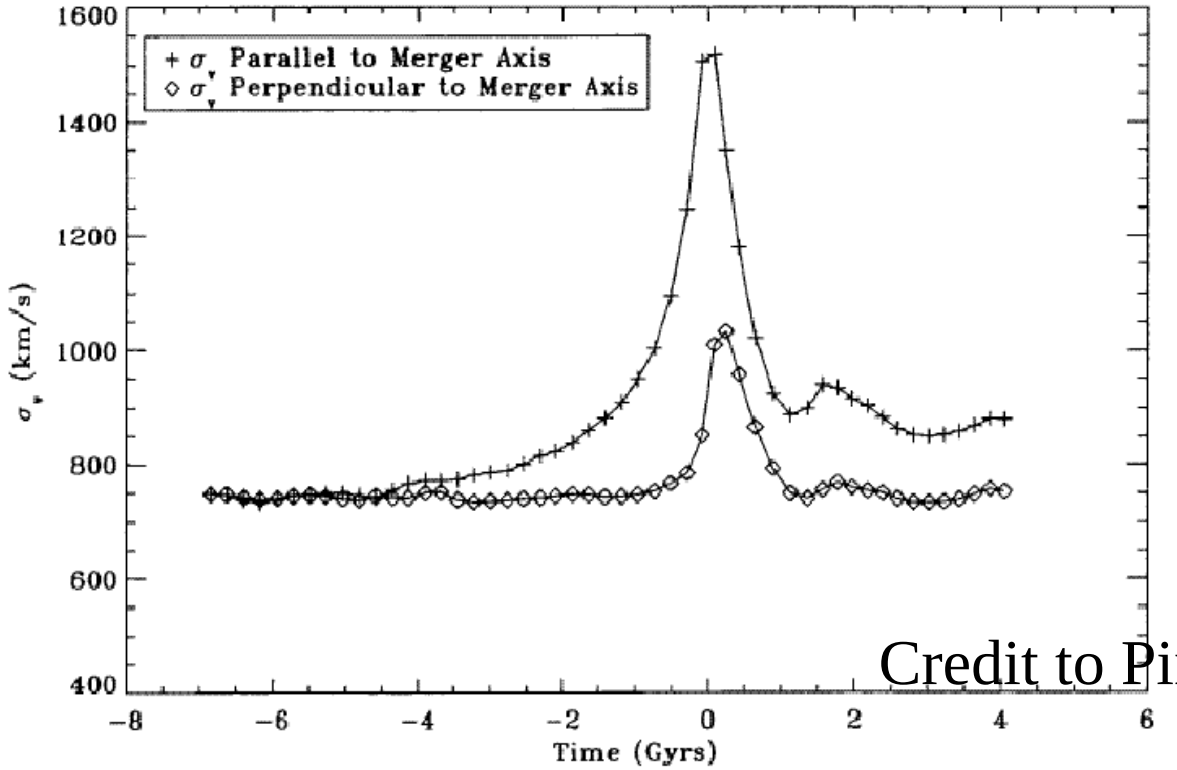

Credit to Pinkney 1996

CLASH-VLT data MACS J0416 at z=0.4
And Abell 209 at z=0.2
3D-analysis. Dessler-Schectman test
For departure of the local mean velocity
From global mean velocity.

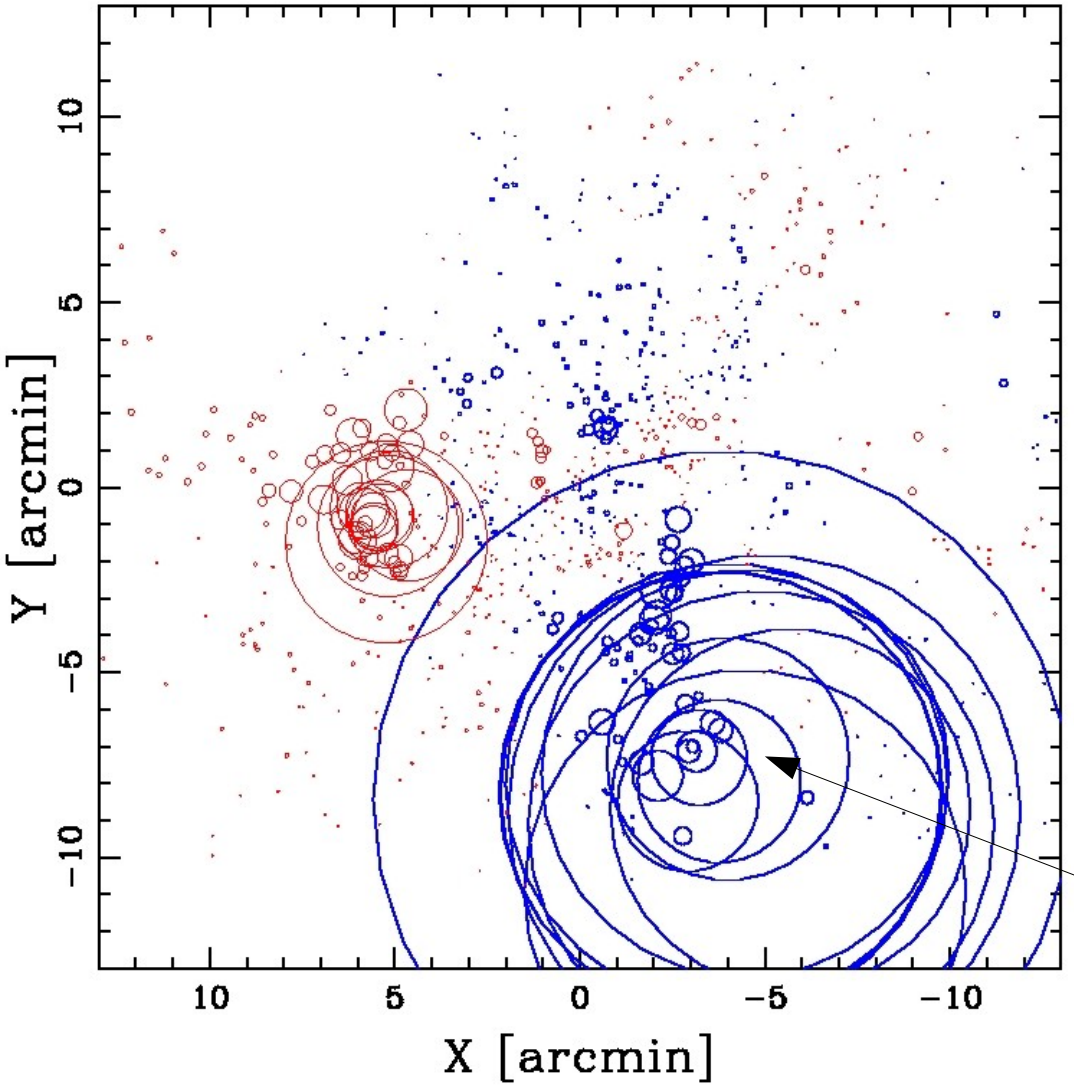

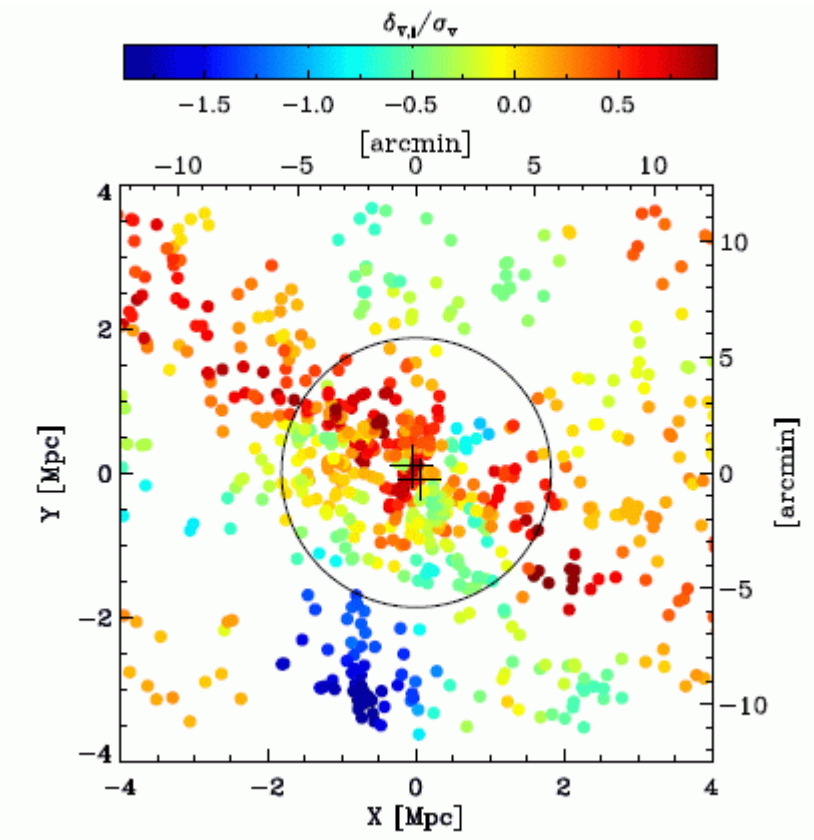

Statistical sign. through
Montecarlo simulations.

Low mean velocity

SOLUTIONS FOR THE TWO BODY HEAD-ON COLLISION CREDIT TO APJ 1984, 286, 422

d) Double Cluster Infall Analysis

The binary nature of the A2197/A2199 system provides a nearly unique opportunity of determining cluster masses independent of the virial technique. The analysis described here was originally outlined by Thompson (1982) and it starts with the formalism introduced by Peebles (1971) and Gunn (1974). The unique character of the following solution lies in the fact that the total system mass and M/L ratio are determined as a function of the projection angle α between the plane of the sky and the line connecting the cluster centers (i.e., $\alpha = 0$ if the two clusters are at precisely the same cosmological distances from the observer). Consequently we find a set of solutions which depend on α.

Let us clearly state that the solution rests on the simplifying assumptions of a simple two-body problem with linear motion (i.e., no rotational support) and boundary values of $R = 0$ at $T = 0$. We start with the well-known parameterized solutions to the field equations, with separate solutions for the bound and unbound cases:

	Bound (SV-ellipse)	Unbound	
$R =$	$\frac{R_m}{2}(1 - \cos\chi)$	$\frac{GM}{v_\infty^2}(\cosh\chi - 1)$	(1)
$T =$	$\left(\frac{R_m^3}{8GM}\right)^{1/2}(\chi - \sin\chi)$	$\frac{GM}{v_\infty^3}(\sinh\chi - \chi)$	(2)
$V =$	$\left(\frac{2GM}{R_m}\right)^{1/2}\frac{\sin\chi}{1 - \cos\chi}$	$V_\infty\frac{\sinh\chi}{\cosh\chi - 1}$.	(3)

The relationship between R_p (the projected separation on the plane of the sky) and R (the true spatial separation) is the simple geometrical equality

$$R_p = R\cos\alpha\,, \tag{4}$$

where $R_p = 6.25/h \times 10^{24}$ cm; and similarly the true relative velocity V and the observed radial velocity V_R are related by

$$V_R = V\sin\alpha\,, \tag{5}$$

where $V_R = 194 \pm 77$ km s^{-1}.

After substituting equations (4) and (5) into equations (1)–(3), it becomes obvious that the problem is overdetermined, and that a

Boschin et al 2010

CREDIT TO ASTRONOMY AND ASTROPHYSICS, BOSCHIN ET AL.

A&A 521, A78 (2010)

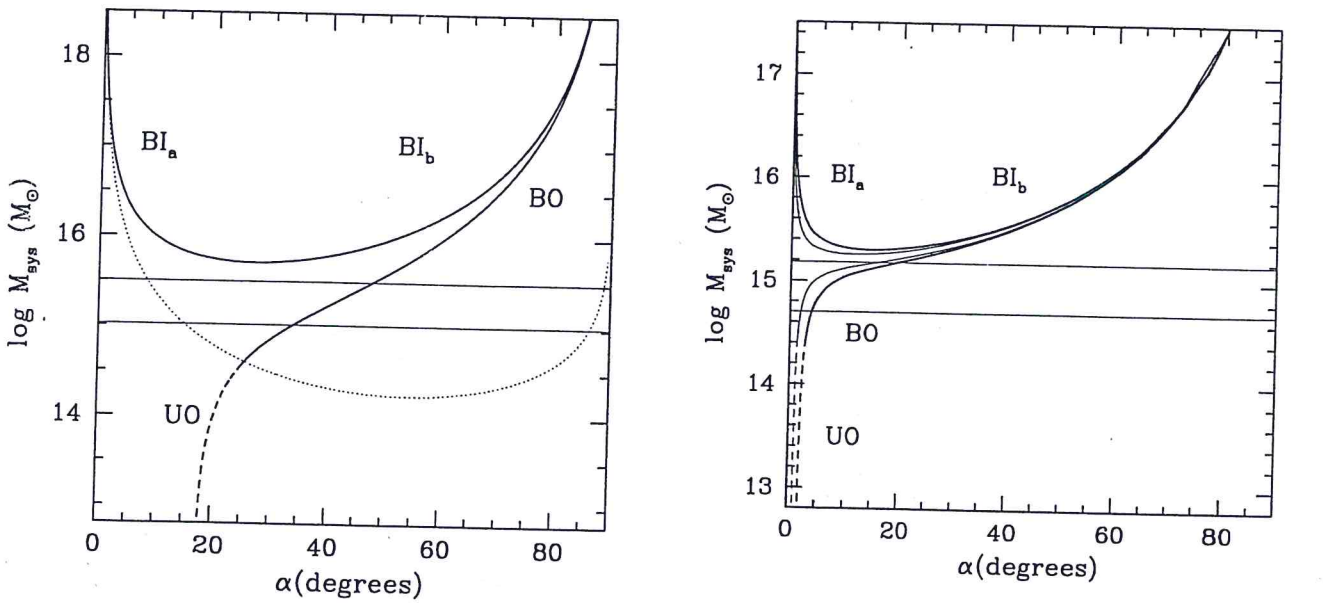

Fig. 11. The same that in Fig. 10 but for the NW and SW subsystems. Thick and thin lines give the results for $V_{rf,LOS} \sim 100$ and 50 km s^{-1}, respectively.

Cluster mergers can stop or enhance the star formation in galaxies.
Debate in the literature.

Caldwell+1993 Post Starbust (PSB) galaxies and cluster mergers

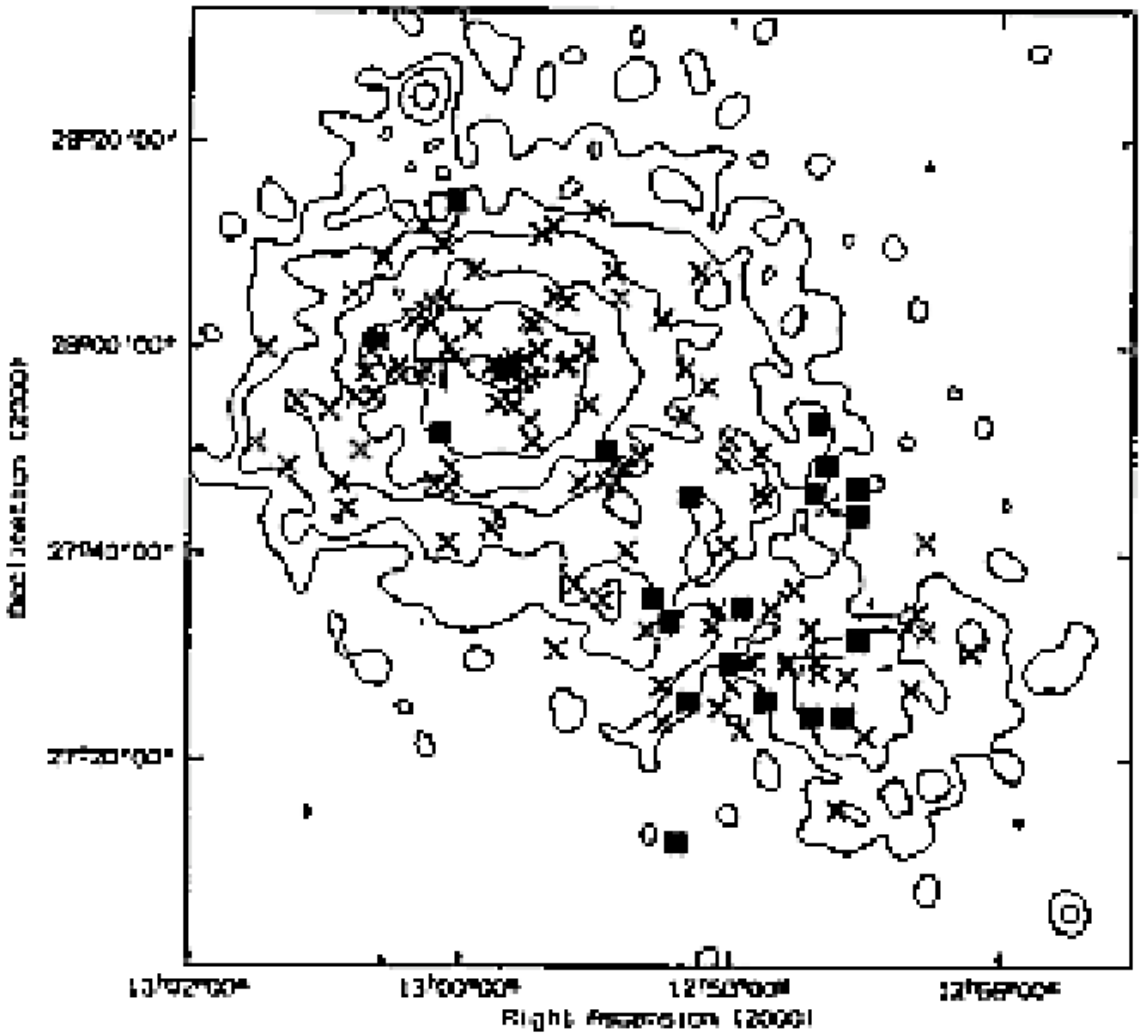

X-ray morphology
Forman 1984
Rosat data.
Surface brightness contours.

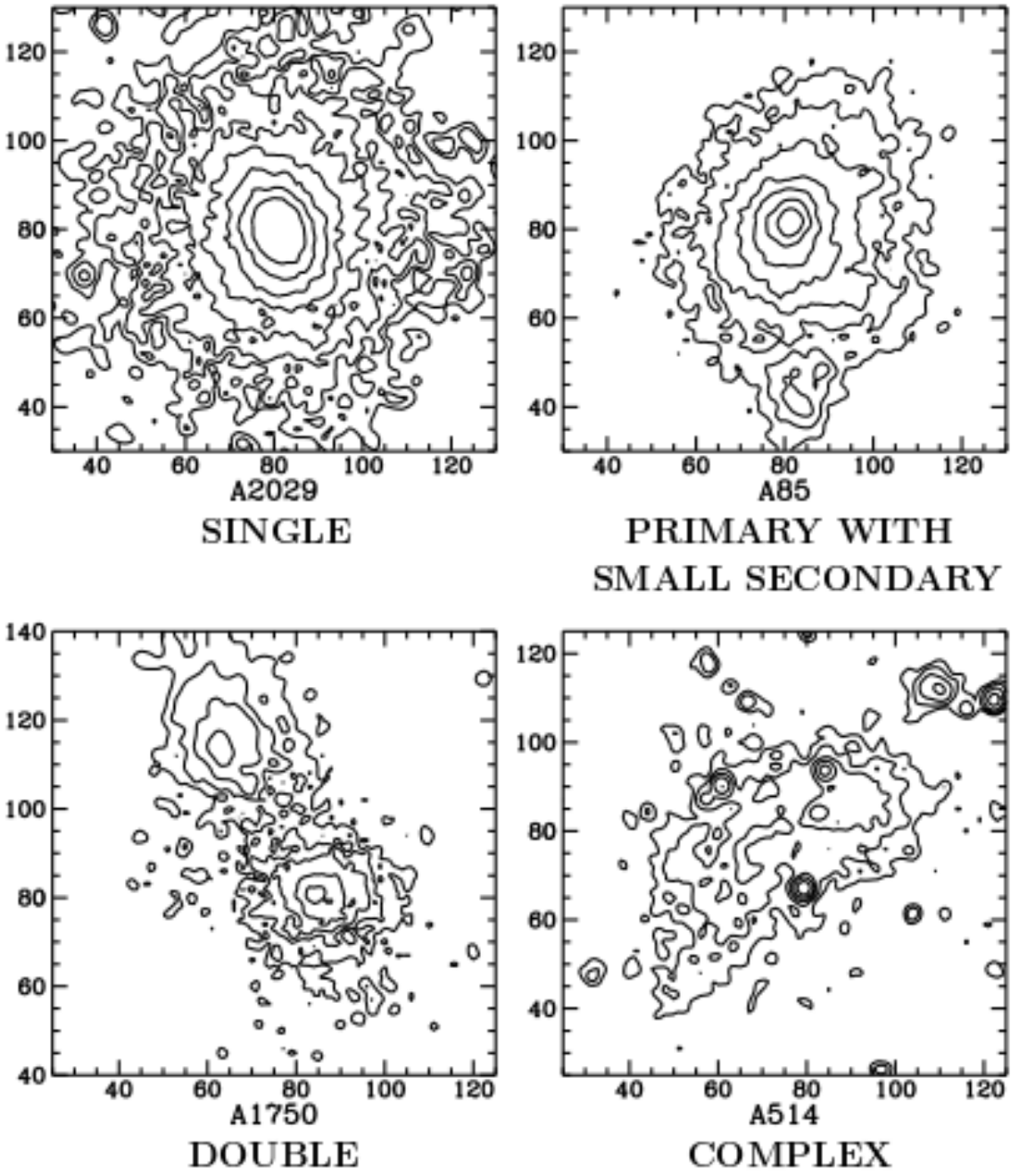

2.1. METHODS

Perhaps the most common approach used to quantify the morphologies of a large number of X-ray cluster images has been with a measure of the X-ray ellipticity (e.g., McMillan et al. 1989; Davis 1994; Mohr et al. 1995; Gómez et al. 1997; Gómez et al. 2000; Kolokotronis et al. 2001). This method is not a particularly good indicator of the dynamical state since both relaxed and disturbed clusters can have significant ellipticity. And even disturbed clusters can have small ellipticity if the substructure is distributed symmetrically about the cluster center. Moreover, even if both the ellipticity and associated position angles are considered they only provide a crude measurement of cluster morphology and have never been shown to provide an interesting distinction between the variety of morphologies exemplified by the Jones & Forman classes.

A better method is the center-shift introduced by Mohr et al. (1993). This popular method has been applied in various forms to X-ray cluster images in several studies (e.g., Mohr et al. 1995; Gómez et al. 1997, 2000; Rizza et al. 1998; Kolokotronis et al. 2001). The basic idea is to divide up a cluster image into a series of circular annuli having different radii but with centers located initially at a guess for the cluster center. The center-shift is then given by the rms difference between the centroid computed for each of these annuli and the weighted average centroid for all annuli.

Since the center-shift is sensitive only to asymmetries in the X-ray images (in particular non-ellipsoidal configurations) it is much more reliable than the ellipticity as an indicator for when a cluster is relaxed. However, it is not transparent how the center shift translates into a physical measure of the dynamical state. And since the center-shift is most sensitive to mergers of equal-mass subclusters, it cannot by itself distinguish the full range of structures exhibited by the Jones & Forman morphological classes.

If the only objective were to distinguish the full range of cluster morphologies then the logical procedure would be to decompose cluster images into a set of orthogonal basis functions of which wavelets (see § 1) are the probably best example. The wavelet coefficients would then define the parameter space of cluster morphologies. Unfortunately, there is no obvious connection (of which I am aware) between wavelet coefficients and a physical measure of the dynamical state.

One method that is both closely related to the cluster dynamical state and provides a quantitative description of the full range of Jones & Forman morphological classes is the "power ratio" method (Buote & Tsai 1995, 1996; Buote 1998). The power ratios are constructed from

the moments of the two-dimensional gravitational potential. Specifically, one evaluates the square of the moments over a circle of radius, R, where the origin is located at the center of mass or at the largest mass peak. The ratio of term, m, to the monopole term is called a "power ratio",

$$\frac{P_m}{P_0} \equiv \frac{\langle (\Psi_m^{\rm int})^2 \rangle}{\langle (\Psi_0^{\rm int})^2 \rangle}, \tag{1}$$

where $\Psi_m^{\rm int}$ is the mth multipole of the two-dimensional gravitational potential due to matter interior to the circle of radius, R, and $\langle \cdots \rangle$ represents the azimuthal average around the circle. In detail we have,

$$P_0 = \left[a_0 \ln (R) \right]^2 , \tag{2}$$

for $m = 0$,

$$P_m = \frac{1}{2m^2 R^{2m}} \left(a_m^2 + b_m^2 \right) \tag{3}$$

for $m > 0$. The moments a_m and b_m are given by,

$$\begin{aligned} a_m(R) &= \int_{R' \leq R} \Sigma(\vec{x}') \, (R')^m \cos m\phi' d^2x', \\ b_m(R) &= \int_{R' \leq R} \Sigma(\vec{x}') \, (R')^m \sin m\phi' d^2x', \end{aligned}$$

where $\vec{x}' = (R', \phi')$.

These ratios are directly related to the 2D gravitational potential if one has a map of the 2D surface mass density such as provided by weak gravitational lensing studies. For X-ray studies Σ is replaced with the X-ray surface brightness, $\Sigma_{\rm x}$, and therefore the power ratios in X-ray studies are really derived from a pseudo potential. These ratios are most sensitive to structures on the same scale as the aperture radius, R.

When the aperture is located at the peak of the X-ray emission the dipole power ratio, P_1/P_0, provides structural information similar to the center shift discussed above (see also Dutta 1995). For an aperture located at the centroid of the surface brightness the dipole moment vanishes. In this case the quadrupole power ratio, P_2/P_0, is sensitive to the degree of flattening and is related to the ellipticity. But unlike ellipticity P_2/P_0 is also sensitive to the radial profile of the X-ray emission.

The primary physical motivation behind the power ratios is that they are related to potential fluctuations. And since it is thought that large potential fluctuations drive violent relaxation in clusters, the power ratios are closely related to the dynamical state of a cluster (Buote 1998). The other motivation is that the multipoles are a complete orthogonal

set of basis functions for the (pseudo) potential and thus are well suited to classify the wide range of observed cluster morphologies.

To get a feel for the power ratios let us see how they behave on the *ROSAT* PSPC images of clusters in the different Jones & Forman morphological classes shown in Figure 3.2. The four clusters inhabit the extreme Jones & Forman classes. A2029 is a smooth, single component system apparently in a relaxed state. A85 has a regular dominant component but with a small structure ~ 0.6 Mpc to the S. A1750 is a double cluster consisting of two roughly equal-sized components separated by ~ 1 Mpc. A514 is a highly irregular aggregation of structures.

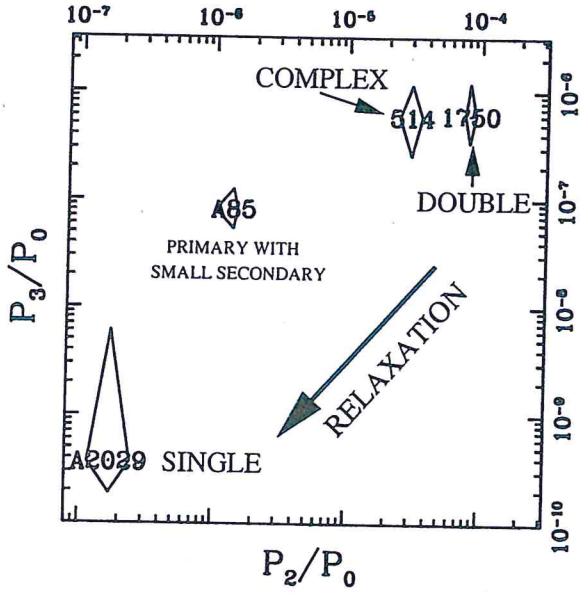

Figure 3.6. Power ratios (from Buote & Tsai 1996) for the clusters in Figure 3.2 computed within a circular aperture of 1 Mpc radius located at the centroid of the X-ray emission.

In Figure 3.6 I show the power ratios, P_2/P_0 and P_3/P_0, of these clusters computed for a 1 Mpc aperture[2] where the aperture is located at the centroid of the X-ray emission (i.e., analog of the center of mass).

Temperature maps overlaid To brightness Isocontours. Bourdin and Mazzotta 2008.

A cool core is a sign of a relaxed cluster.

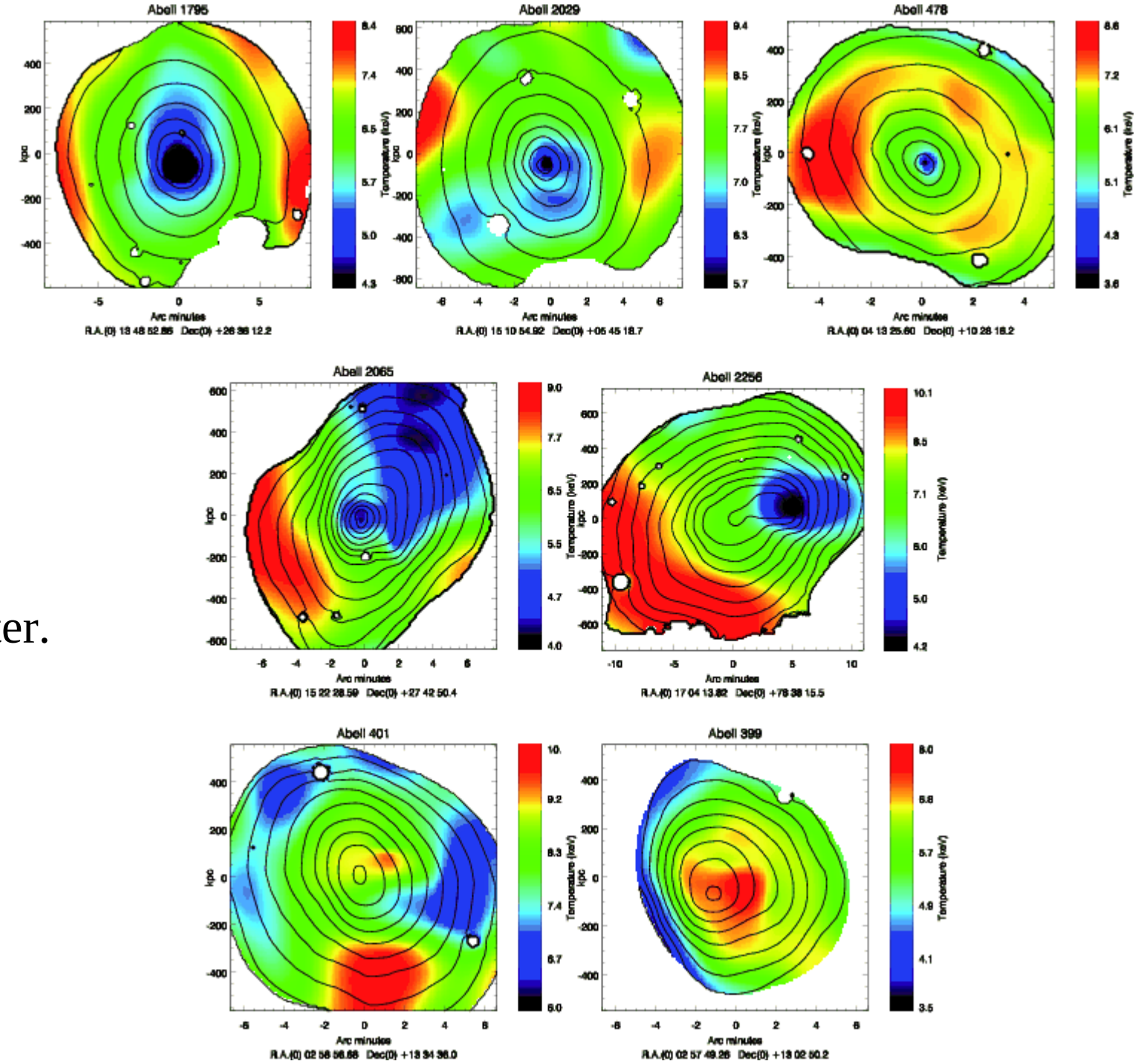

Buote 2002. A scenario for cluster evolution.

Now
Cool core
Not cooling flows.

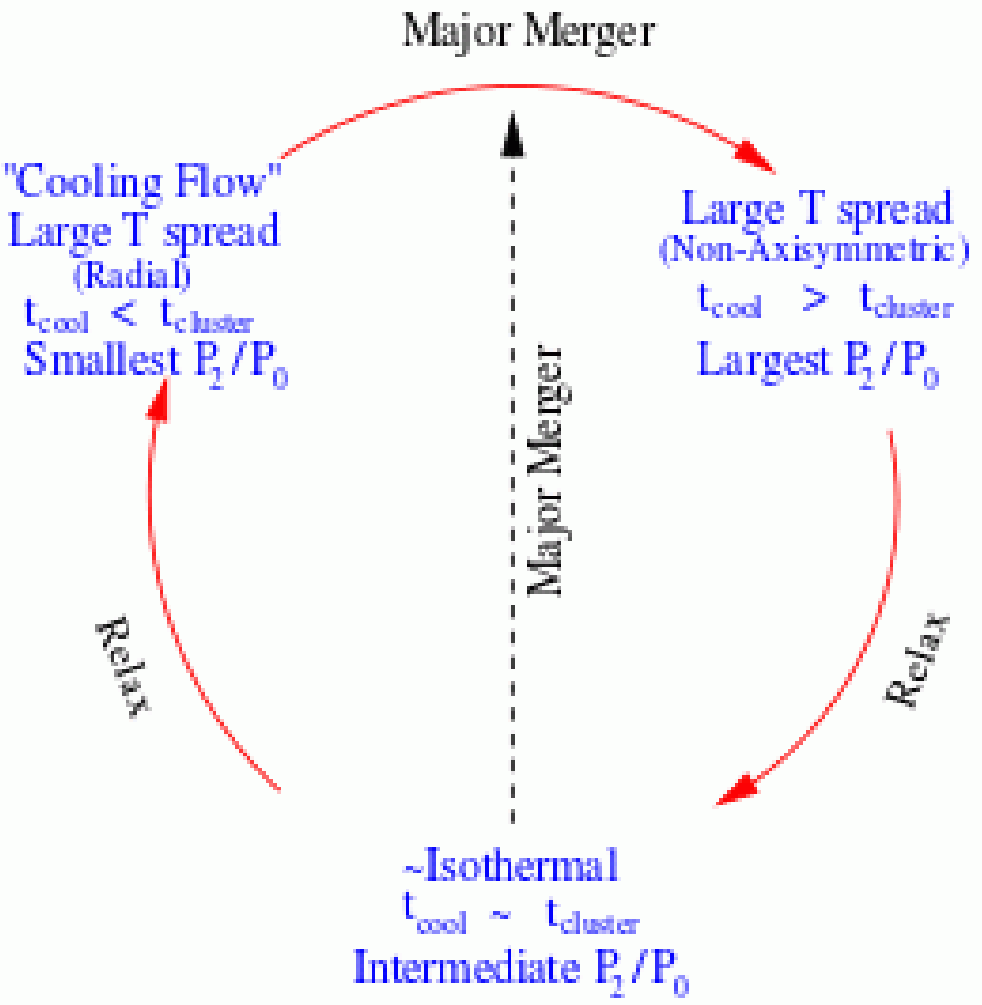

Figure 1.17. A possible description of the evolution of the X-ray temperature structure and image morphology during the formation and evolution of a cluster.

A2219, z~0.22
Radio halo

(Boschin, MG, Barrena, et al. 2004, AA, 416, 839)
TNG/Dolores +CFHT multiobject spectroscopy
SE-NW cluster and cD elongation

σ_v ~1400 kms-1

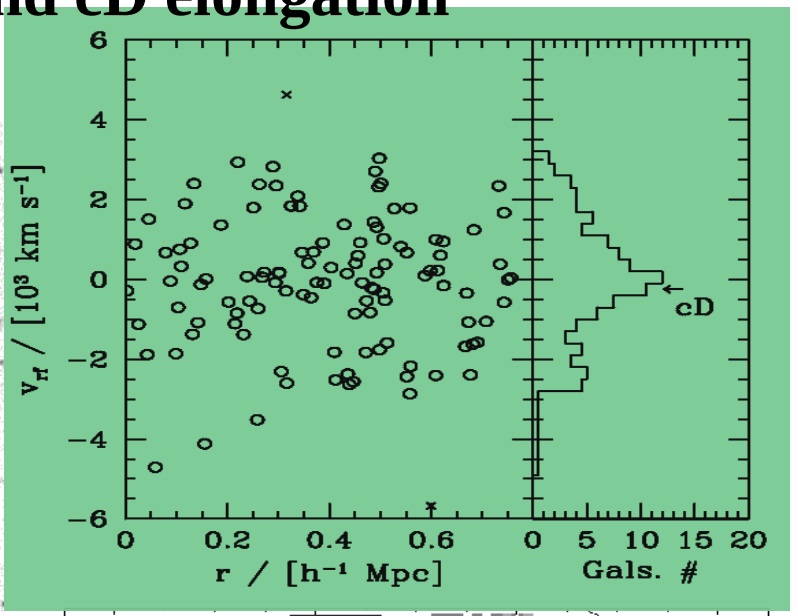

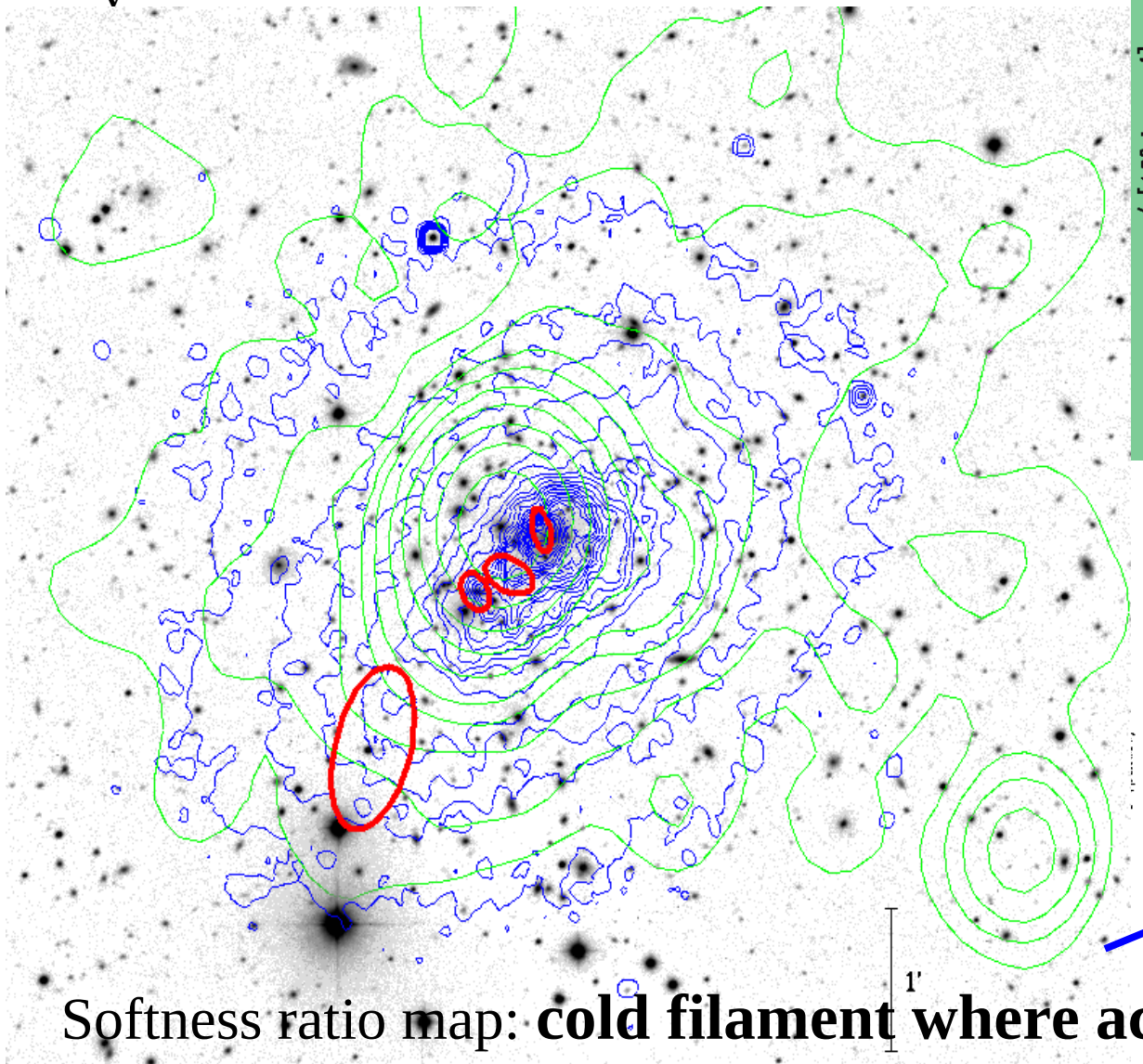

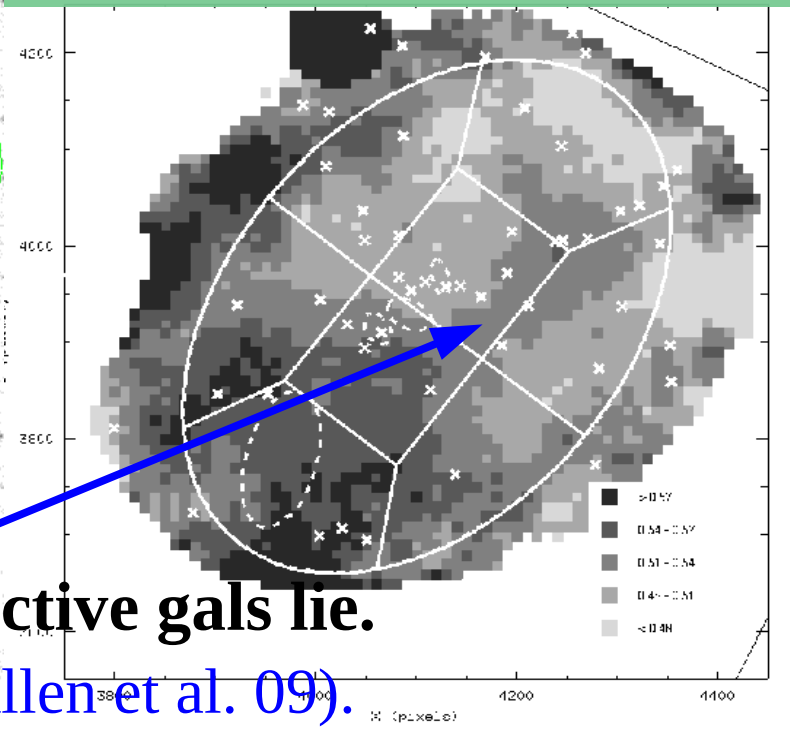

Softness ratio map: **cold filament where active gals lie.**

Recent discover of a cold front (Million & Allen et al. 09).